

Contents list available at CBIORE journal website

International Journal of Renewable Energy Development

Journal homepage: https://ijred.cbiore.id



Research Article

Response surface optimization of biodiesel synthesis from crude palm oil (CPO) using CaO/silica gel heterogeneous catalyst based on blood cockle shell and coconut fiber

Nurhayati Nurhayatia* , Amir Awaluddin , Yenni Mulyanib

Abstract. This study successfully synthesized a hybrid catalyst CaO-silica gel from environmentally friendly raw materials, CaO derived from blood clam shells and silica gel obtained from coconut fiber waste ash. The catalytic activity was evaluated in the synthesis of biodiesel from crude palm oil (CPO). The CaO-Silica gel catalyst was synthesized by the wet impregnation method with variations of silica gel, namely 5, 10 and 15 wt%. The catalyst was characterized using XRD, XRF, SEM, and BET analysis. The results showed a decrease in CaO content with increasing silica gel concentration, while XRD analysis confirmed the presence of lime, portlandite, Ca₂SiO₄, and silica oxide minerals. The addition of silica gel reduced the crystal size and crystallinity and increased the surface area of the catalyst. Optimization of biodiesel production was carried out using the Response Surface Methodology (RSM), considering variables such as temperature, reaction time, molar ratio of oil to methanol, and catalyst loading. The highest biodiesel yield was obtained using 5% CaO/silica gel catalyst at a temperature of 65°C, a reaction time of 60 minutes, an oil-methanol molar ratio of 1:9, and a catalyst addition of 2%, resulting in a biodiesel yield of 99.52%. In addition, the methyl ester content reached 99.21% using a 10% CaO/silica gel catalyst. The resulting biodiesel met ASTM and EN standards, except for the acid value.

Keywords: Calcium oxide; Silica gel; Crude palm oil; Biodiesel; Response surface methodology (RSM).



@ The author(s). Published by CBIORE. This is an open access article under the CC BY-SA license (http://creativecommons.org/licenses/by-sa/4.0/). Received: 7th Nov 2024; Revised: 5th January 2025; Accepted: 27th January 2025; Available online: 15th Feb 2025

1. Introduction

Energy is a major factor that is crucial to support the economic progress of any country, as all sectors in a country can only operate with a reliable source of energy. However, increasing global energy demand has shown that nonrenewable energy sources such as coal and petroleum have limitations and will run out eventually (Ayoola et al., 2020). In Indonesia, the demand for petroleum-based fuels has reached 93.8% of the transport sector in 2021 (Wirawan et al., 2024). In overcoming this problem, alternative fuels such as biodiesel are widely used as auxiliary fuels for diesel engines. This is due to several advantages, such as clean combustion, biodegradability, low toxicity, less CO2 and CO emissions, ability to be blended with other energy sources, and renewability (Kedir et al., 2023). Indonesia has initiated the utilisation of biodiesel by adopting the national standard B35, which consists of a blend of 35% biodiesel and 65% diesel fuel (Wirawan et al., 2024). Biodiesel is a monoalkyl ester of long-chain fatty acids, synthesized through a transesterification reaction involving triglycerides derived from vegetable oils, animal fats, or waste oils, and short-chain alcohols in the presence of a catalyst (Aibuedefe et al., 2023).

Strong base catalysts such as CaO are commonly used catalysts to maximise transesterification reactions because they

are abundant in nature, cheap, durable, and have high active sites but their stability is not good in transesterification reactions due to the dissolution of Ca2+ ions (Manurung et al., 2023), especially when used on raw materials with high Free Fatty Acid (FFA) content (Ooi et al., 2021). Recent research utilizes biomass waste to produce environmentally friendly catalysts (Manurung et al., 2023). Blood clam shell waste has the potential as a source of CaO, with CaCO3 content that decomposed up to 97.834% through calcination at 900°C for 5 hours (Nurhayati et al., 2020). Biodiesel production using blood clam shell CaO catalyst with crude palm oil (CPO) raw material has been carried out (Maisarah et al., 2020) and the results reached 77.89%, but the purity of biodiesel is still low because of the formation of emulsions due to CPO containing high FFA (>5%) (Nurhayati et al., 2020). Nevertheless, efforts to maximise CPO as a biodiesel raw material need to be made considering that Indonesia is the world's largest CPO producer, where in 2021 CPO production will reach 48 million tonnes (Wirawan et al., 2024). One of the efforts made is to modify CaO with silica which has a high surface area and good thermal stability, which can increase the stability and reactivity of CaO (Ozor et al., 2023). Solid acid

^a Department of Chemistry, Faculty of Mathematics and Natural Sciences, Riau University, Pekanbaru 28293, Indonesia

 $[^]b$ Master Program of Chemistry, Faculty of Mathematics and Natural Sciences, Riau University, Pekanbaru 28293, Indonesia

^{*} Corresponding author

catalysts such as silica have the potential to produce biodiesel from oils containing high FFA (Sofyan *et al.*, 2024).

Silica can be extracted from biomass waste ash through various methods, with the sol-gel technique being one of the common approaches to form silica gel. Silica gel extraction yields include 68.28% from palm frond ash (Osman & Apawe, 2020), 95.35% from rice husk ash (Setyawan et al., 2021), 95.9% from palm kernel shell ash (Manurung et al., 2023), 89.57% from coconut husk ash and 94.89% from coconut shells (Pattanayak et al., 2022), and 75.58% from coconut husk fiber (Norul Azlin & Syamim Syufiana, 2022). Previous research has utilized the wet impregnation method to synthesize CaO/SiO₂ catalysts, with CaO sourced from chicken eggshells and silica from rice husk ash, resulting in a biodiesel yield of 98.65% from palm oil. Furthermore, this catalyst exhibited high stability, maintaining its activity over five cycles with minimal yield reduction (Lani et al., 2020). Other studies have combined CaO with silica gel, such as using CaO from local limestone and silica from rice husk ash for transesterification of coconut oil, achieving a 98.3% biodiesel yield (Pandiangan et al., 2019). Similarly, silica gel from palm kernel shell ash and CaO from chicken eggshell were used to synthesize biodiesel from palm oil, with a yield of 97% (Manurung et al., 2023). Additionally, a catalyst composed of CaO from Java duck eggshells modified with silica gel from rice husk ash was tested for its catalytic activity in biodiesel production, yielding 81.4% biodiesel (Haryono et al., 2023).

This modification is proven to increase the stability of the CaO catalyst, prevent the formation of Ca²⁺, and increase the biodiesel yield to the range of 81-98.3% (Pandiangan *et al.*, 2019; Lani *et al.*, 2020; Manurung *et al.*, 2023; Haryono *et al.*, 2023). This condition is caused by the addition of silica, especially in the form of silica gel, which has a high surface area (Sofyan *et al.*, 2024). The incorporating of silica gel from rice husk ash can increase the surface area of CaO from blood clam shells from 1.36 m²/g to 9.47 m²/g (Lani *et al.*, 2020). The silica not only increases the stability of CaO by preventing the formation of Ca²⁺, but also increases its reactivity (Ozor *et al.*, 2023).

Silica sources exhibit varying effects on enhancing the activity of CaO catalysts, influenced by their unique characteristics. While rice husk ash and palm kernel shell ash have been commonly utilized as silica sources in previous studies (Lani et al., 2020; Manurung et al., 2023). Coconut husk ash, containing 91.76% silica predominantly in the form of silica gel (Anuar et al., 2020), represents a promising alternative. However, until now, the use of silica gel from coconut husk ash as an additive to modify CaO catalysts has not been reported in previous studies. In this study, silica gel from coconut coir ash was used to modify CaO from blood clam shells to improve catalyst activity in the synthesis of biodiesel from CPO.

In addition to modifying the catalyst, optimal biodiesel yields can also be achieved by conducting experimental designs that explore various reaction variables. Response Methodology (RSM) is a widely used as a statistical tool for optimizing process parameters in biodiesel production. When combined with Central Composite Design (CCD), RSM allows for a more effective study of the interactions between variables such as the methanol to oil molar ratio, catalyst concentration, temperature, and reaction time. This approach not only minimizes the number of experiments needed but also provides graphical representations of how these variables and their interactions affect the response, aiding in the determination of the optimal conditions for maximizing biodiesel yield. Previous studies have demonstrated the effectiveness of RSM in improving biodiesel production efficiency under various transesterification conditions. Researchers

Krishnamurthy *et al.* (2020), Buasri *et al.* (2024), Ahmed *et al.* (2023), and Ahamed *et al.* (2023) have successfully used RSM to optimize process variables, leading to high biodiesel yields.

2. Materials and Methods

2.1 Materials

The materials used in this study include crude palm oil taken from PT Kuala Lumpur Kepong Berhad in Dumai City, as well as blood clam shells obtained from various seafood restaurants in Pekanbaru. and coconut husk from Kuantan Singingi Regency, CH₃OH (Merck), hydrochloric acid (HCl) (Smart Lab), NaOH (Merck), CH3COOH (Merck), Whatman 42 filter paper, Aqua DM.

2.2 Methods

2.2.1. Preparation of CaO Catalyst

The CaO catalyst was prepared from blood cockle shells through a series of steps to ensure purity and efficiency. First, the shells were cleaned and soaked overnight in a 2% acetic acid solution (table vinegar) to remove impurities. After rinsing thoroughly using distilled water, the shells were dried at 105°C for 24 hours The dried shells were then crushed, sieved through a 200-mesh screen, and calcined at 900°C for 5 hours (Nurhayati et al., 2020). The calcination conditions were selected based on previous studies to achieve optimal crystallinity and catalytic activity.

2.2.2. Synthesis of Silica Gel

The synthesis of silica gel was conducted in two primary stages: the extraction of SiO₂ from coconut husk and the subsequent formation of silica gel, with the procedures adapted from the methods described by Lani et al. (2017) and Pattanayak et al. (2022). The initial stage involved the preparation of raw materials, wherein coconut husk was cut into small pieces, washed with distilled water and sun-dried to achieve complete dryness. The dried coconut fiber was calcined at 700°C for 2 hours to obtain ash containing silica. Subsequently, 10 grams of the resulting ash was dissolved in 100 mL of 3N HCl solution and heated to 110°C for 5 minutes. The heat source was then turned off, allowing the temperature to decrease to 80°C, and continuously stirred for 1 hour. The second stage focused on gel formation. In this process, 5 grams of SiO₂ from the previous stage was combined with 50 mL of 3.5N NaOH solution in a reflux system. The mixture was heated at 100°C for 1 hour to achieve a homogeneous solution. The resulting filtrate from this process was then added with with 1N HCl solution until a gel formed and the pH was adjusted to 7. The formed gel was aged for 18 hours to enhance its structural stability. Then, the gel was washed with distilled water and dried in an oven at 70°C, sieved using 200-mesh and stored for use in the subsequent catalyst synthesis stage.

2.2.3. Synthesis of CaO/Silica Gel Catalyst

The synthesis of the CaO/silica gel catalyst was conducted using the wet impregnation method, with modifications based on the procedure described by Haryono *et al.* (2023). Initially, 10 g of CaO was suspended in 100 mL of distilled water and stirred until a homogeneous mixture was achieved. The suspension was then transferred to a three-neck flask. Silica gel powder was added to the suspension in varying proportions of 5%, 10%, and 15% (w/w). The resulting mixture was refluxed at 80°C for 4 hours to promote optimal interaction between CaO

 Table 1

 Relationship between independent variables and variable code

Variable	Unit	Coding -	Range and Level					
	Oilit	Couling -	-α	-1	0	+1	+α	
Reaction Temperature	°C	Α	50	55	60	65	70	
Reaction time	minute	В	30	60	90	120	150	
Molar ratio of methanol to oil	-	С	6:1	9:1	12:1	15:1	18:1	
Catalyst loading	(wt%)	D	0.5	1	1.5	2	2.5	

and silica gel. Following reflux, the mixture was dried at 105°C for approximately 24 hours to eliminate residual moisture. Finally, the dried product was calcined 3 h at 800°C in a furnace to activate the catalyst.

2.2.4. Experimental Design with RSM

The synthesis of biodiesel from CPO was studied by analyzing the effect of parametric variables on the process, utilizing analysis of variance and optimization through Response Surface Methodology (RSM). A Central Composite Design (CCD) was used to evaluate the influence of four independent variables on the yield of methyl esters, which served as the dependent variable and primary response. The optimization focused on key transesterification process variables: reaction temperature (A), reaction time (B), molar ratio of methanol to oil (C), and catalyst amount (D). The range and levels of these independent variables, along with their actual values and coded representations, are presented in Table 1.

Determination of optimimal condition of biodiesel synthesis process conditions using RSM based on the table was entered into the design expert 12 application to obtain the experimental design of the CaO/Silica gel catalyst and variable codes that have been determined. A total of 30 experiments were conducted, comprising 16 factorial points (2⁴), 8 axial points (K = 4 independent variables with 5 levels), and 6 midpoint replications to estimate experimental error.

2.2.5. Biodiesel Synthesis

Biodiesel was synthesized using a 500 mL round-bottom flask. Initially, 100 g of CPO was preheated to 105°C for 30 minutes to remove moisture. The CPO was then allowed to cool to 50°C. In a separate flask, the catalyst was combined with

methanol in the flask and refluxed for 1 hour. The cooled CPO (50°C) was added to the filtered methanol and refluxed under specific conditions of temperature and time as determined by the RSM optimization. The reaction was conducted with continuous stirring at 500 rpm to ensure proper mixing. The reaction mixture was placed in a separatory funnel and left to settle for the night. The resulting biodiesel was filtered and washed with demineralized water (aqua DM) at 60°C. The mixture was then shaken and allowed to stand overnight to facilitate phase separation, the upper, light-colored layer consisting of biodiesel, and the lower, milky-white layer comprising an emulsion of soap, methanol, and washing water. The biodiesel was then collected, dried by heating, and weighed. The biodiesel yield was calculated using the following equation:

Yield biodiesel (%) =
$$\frac{\text{weight of biodiesel(g)}}{\text{weight of oil (g)}} \times 100\%$$
 (1)

The synthesized biodiesel properties were evaluated following the guidelines of ASTM D6751 and EN 14214 standards, encompassing parameters such as density, viscosity, carbon residue, moisture content, acid value, while the composition and purity analysis of biodiesel were determined using GC-MS.

3. Results and Discussion

3.1 Composition Analysis

Quantitative elemental analysis using XRF showed the composition of silica gel, CaO, and CaO/silica gel (5%, 10%, 15%) listed in Table 2. Silica gel contains SiO_2 (92.965%) and

Table 2
Chemical composition analysis results of silica gel catalyst, CaO, CaO/silica gel (5%, 10%, and 15%)

Composition —	Content (%)								
	Silica gel	CaO	CaO/silica gel 5%	CaO/silica gel 10%	CaO/silica gel 15%				
CaO	0.697	98.142	95.799	94.970	91.139				
SiO_2	92.965	0	1.558	3.087	6.743				
Al_2O_3	0.911	0.301	0.300	0.474	0.567				
P_2O_5	2.823	0.702	0.823	0.784	0.874				
Fe_2O_3	0.082	0.013	0.021	0.044	0.020				
MnO	0.003	0.028	0.034	0.034	0.032				
Cl	2.342	0.004	0.054	0.079	0.069				
V_2O_5	0.001	0.006	0	0.002	0.001				
SrO	0	0.293	0.209	0.220	0.213				
Ag_2O	0	0.509	0	0,288	0.314				
ZrO_2	0.003	0.002	0	0	0				
TiO_2	0.049	0	0.002	0.012	0.012				
ZnO	0.055	0	0.004	0.005	0.006				
CuO	0.003	0	0.005	0	0.003				
BaO	0	0	0.005	0	0.006				
K_2O	0.065	0	0	0	0				

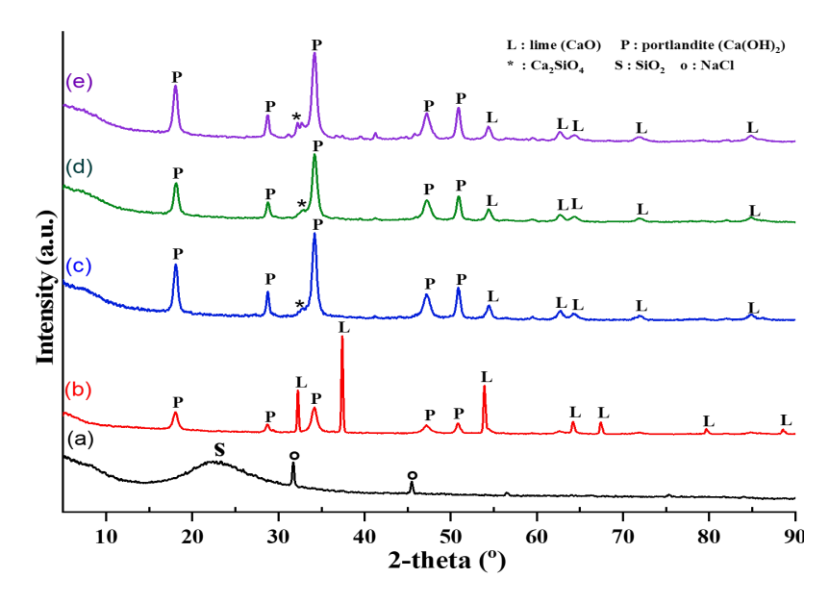


Fig. 1. XRD diffractograms of (a) Silica gel, (b) CaO, (c) CaO/silica gel 5%, (d) CaO/silica gel 10%, and (e) CaO/silica gel 15%

several other elements such as P_2O_5 , Cl, Al_2O_3 , and Fe_2O_3 . This silica content is quite high compared to commercial silica (95.37%) (Setyawan *et al.*, 2021) as well as previously reported silica from coconut fibre (91.76%) (Anuar *et al.*, 2020). This suggests that coconut husk ash has potential as a source of silica. The percentage of CaO from blood clam shells was 98.142%, slightly higher than that reported (97.834%) (Nurhayati *et al.*, 2020), and close to the commercial CaO content (99%) (Wongjaikham *et al.*, 2023).

After impregnation with silica gel, the CaO content decreased while the SiO₂ content increased. At CaO/silica gel 5%, 10%, and 15 % catalysts, the CaO content was 95.799% 94.970% and 91.139%, respectively, while the SiO₂ content was 1.558%; 3.087%; and 6.743%. The highest CaO percentage was found in CaO/silica gel 5%, and the highest SiO₂ in CaO/silica gel 15%. This modification aims to increase the stability and reactivity of CaO with the help of surface area and thermal stability of silica gel (Sofyan *et al.*, 2024). The decrease in CaO percentage and increase in SiO₂ indicate the success of silica gel impregnation on CaO, which is influenced by the optimal impregnation process (Haryono *et al.*, 2023; Hadiyanto *et al.* 2016).

3.2 Mineral type, crystal size, and crystallinity of catalysts

Silica gel, CaO, and CaO/silica gel catalysts (5%, 10%, and 15%) were characterized using XRD to identify mineral phases, crystal sizes, and crystallinity. The diffractograms obtained at 2θ angles ranging from 10° to 90° were compared to JCPDS standards (Figure 1). The observed peaks revealed the presence of lime (CaO), portlandite (Ca(OH)₂), calcium silicate (Ca₂SiO₄), coesite (SiO₂), and halite (NaCl) minerals. The diffractogram of silica gel (Figure 1a) exhibits an amorphous nature, characterized by broad peaks between $2\theta = 15^{\circ}-30^{\circ}$ and a

maximum intensity at $2\theta=22^\circ$, indicating the absence of a well-defined crystal structure. Similar results were also reported by Alhadhrami *et al.* (2022), Zuwanna et al. (2023), and Lani *et al.*, (2017). However, the presence of sharp peaks at $2\theta=31.74^\circ$ and 45.43° suggests the presence of NaCl impurities, likely resulting from an incomplete leaching process, as similarly observed in studies by Ghadafi *et al.* (2020) and Pattanayak *et al.* (2022).

The diffractogram of CaO (Figure 1.b) shows intense peaks at 2θ 32.23° ; 37.36° ; 53.86° ; 64.16° ; 67.39° ; 79.69° ; 88.51° , indicating the presence of CaO. In addition, the presence of Ca(OH)₂ peaks at 2θ 18.05° ; 28.61° ; 34.22° ; 47.18° ; 50.89° indicates the formation of portlandite due to exposure to air, which is in line with research Lani *et al.* (2020). The calcination process at 900° C for 5 hours proved successful in decomposing calcite (CaCO₃) into lime (CaO). In the diffractograms of CaO/silica gel (5%, 10%, and 15%) (Figure 1.c, d, e), there is a peak change from CaO to Ca(OH)₂ at 2θ 34.20° due to reaction with water during impregnation, as reported by Helwani *et al.* (2020). New peaks at 2θ 32.84° ; 32.75° ; and 32.70° indicate the Ca₂SiO₄ phase, which is most evident in the 15% CaO/silica gel catalyst.

The average crystal size and crystallinity (Table 3) were evaluated using the Debye-Scherrer equation. The CaO crystal size before impregnation was 57.515 nm with a crystallinity of 48.754%, indicating low surface area and high crystallinity (Khazaai *et al.*, 2021). Silica gel showed the lowest crystallinity (13.031%), indicating amorphous nature, while the high crystal size (31.579 nm) was due to NaCl impurity. After impregnation, the crystal sizes of CaO/silica gel (5%, 10%, 15%) were 20.883; 19.523; and 30.479 nm, respectively, with crystallinity of 37.847%; 40.084%; and 38.042%, respectively. The smallest crystal size was found with CaO/silica gel 10%, but increased

Table 3Average crystal size and crystallinity of silica gel, CaO, and CaO/silica gel (5%, 10%, and 15%)

Catalyst	Average of crystal size (nm)	Crystallinity (%)
Silica gel	31.579	13.031
CaO	57.515	48.754
CaO/silica gel 5%	20.883	37.847
CaO/silica gel 10%	19.523	40.084
CaO/silica gel 15%	30.479	38.042

Table 4. Specific surface area analysis results, of silica gel, CaO, and CaO/silica gel (5%, 10%, and 15%)

<u></u>	g : : : : : : : : : : : : : : : : : : :		
Material	Surface Area (m²/g)	Total pore volume (cm ³ /g)	Average pore diameter (nm)
Silica gel	186.570	0.863	9.261
CaO	1.032	0.006	12.490
CaO/silica gel 5%	6.097	0.017	5.888
CaO/silica gel 10%	7.695	0.084	22.071
CaO/silica gel 15%	5.866	0.018	6.330

with 15% silica gel addition. This is due to the non-optimal distribution of silica, causing clumping on the catalyst surface, even though the silica in CaO/silica gel 15% has the highest percentage (6.743%).

3.3 Surface Area Analysis

The specific surface area of the catalyst was analyzed using a Surface Area Analyzer (SAA) based on the Brunauer-Emmett-Teller (BET) method, which is based on the principle of nitrogen gas adsorption at 77 K. Adsorption isotherm measurements

0.2

0.4 Relative Pressure, P/Po

were performed using a Surface Area Analyser (SAA), the results of which include the surface area, pore volume, and pore diameter of silica gel and CaO/silica gel (5%, 10%, and 15%) shown in Table 4. The surface area of CaO obtained from blood clam shell waste was 1.03 m²/g, which is lower than that of commercial CaO (3 m²/g), as reported by Putra (Putra et al., 2017), but almost the same as that of CaO from cockle shell of 1.36 m²/g (Lani et al., 2020), indicating a low surface area of CaO from shell waste.

Modification by impregnation of silica gel from coconut coir ash, which has a surface area of 186.570 m²/g (higher than

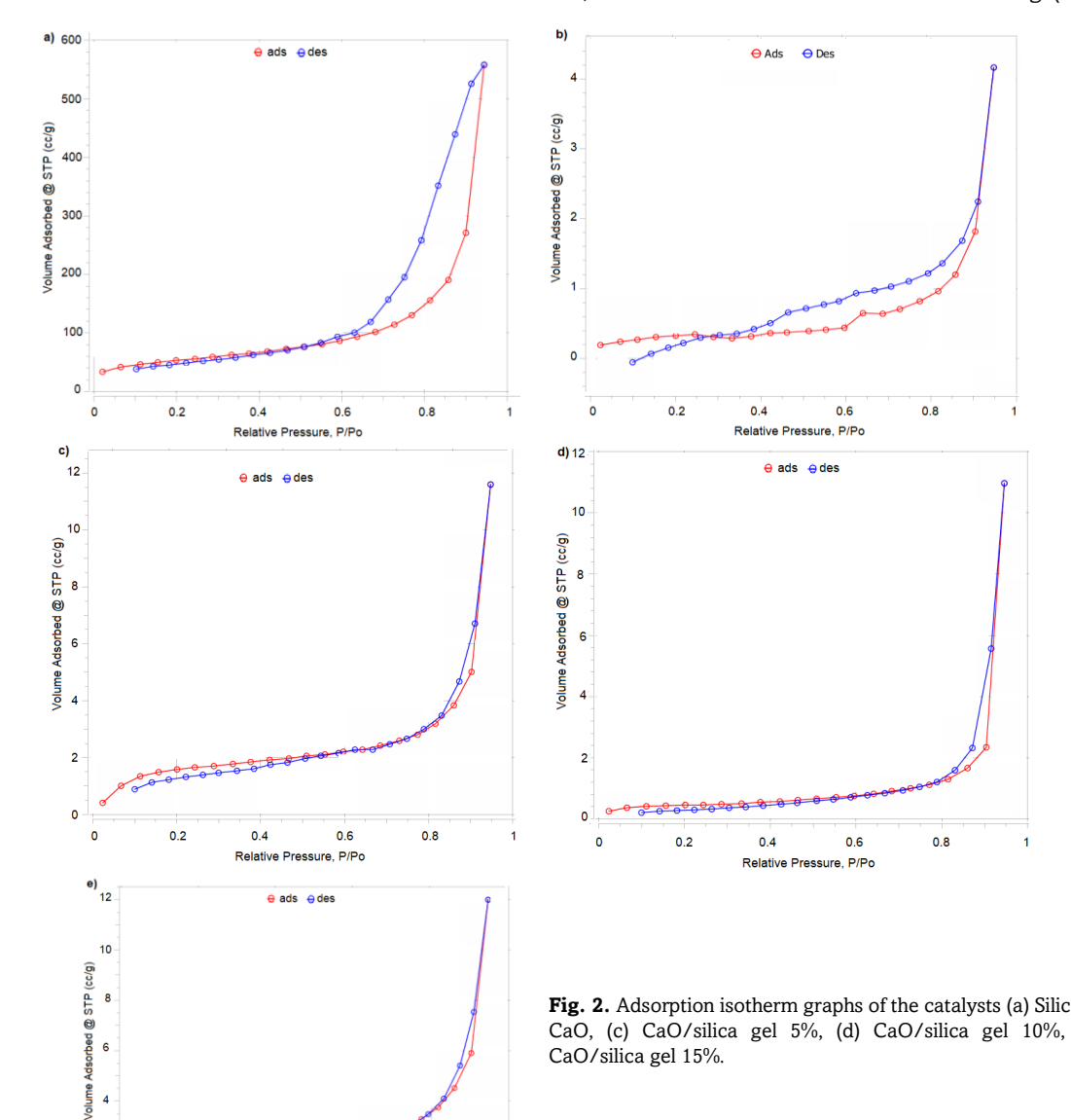
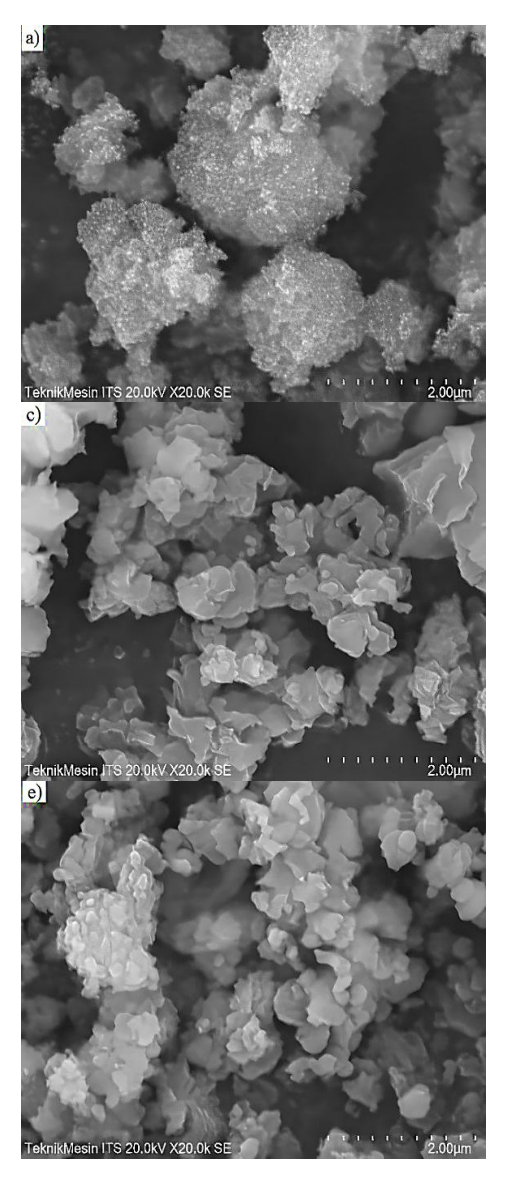


Fig. 2. Adsorption isotherm graphs of the catalysts (a) Silica gel, (b) CaO, (c) CaO/silica gel 5%, (d) CaO/silica gel 10%, and (e) CaO/silica gel 15%.

commercial silica gel of 143.95 m²/g) (Setyawan et al., 2021), successfully increased the surface area of CaO to 6.097 m²/g with the addition of 5% silica gel, and 7.695 m²/g with the addition of 10% silica gel. This increase indicates a strong interaction between CaO and silica that inhibits sintering and stabilizes the CaO surface (Wan Omar & Amin, 2011). However, at the addition of 15% silica gel there is a decrease in surface area thought to be due to non-optimal distribution of silica, which may cover or block access to active sites (Lani et al., 2020). A large surface area increases the possibility of interaction between reactant molecules and catalyst active sites in the transesterification reaction (Simpen et al., 2021). The CaO/silica gel 10% catalyst showed the highest surface area compared to the other catalysts, which might contribute to better catalytic performance. This is consistent with the XRD data, where larger crystal size correlates with smaller surface

The total pore volume of silica gel is 0.863 cm³/g, whereas CaO exhibits a significantly lower pore volume of 0.006 cm³/g. Upon impregnation with silica gel, the pore volume of CaO increases to 0.017 cm³/g with 5% silica gel, reaches a maximum of 0.084 cm³/g with 10% silica gel, and subsequently decreases to 0.018 cm³/g when 15% silica gel is added. The reduction observed at 15% silica gel is attributed to the suboptimal

distribution of silica, which may obstruct access to the catalyst's active sites (Manurung et al., 2023). A higher pore volume enhances the catalyst's ability to adsorb reactant molecules, thereby improving the likelihood of chemical reactions occurring within the pores (Lani et al., 2017). The average pore diameter of silica gel is 9.261 nm, while that of CaO is 12.490 nm. For CaO impregnated with silica gel, the average pore diameters were measured as 5.888 nm with 5% silica gel, 22.071 nm with 10% silica gel, and 6.330 nm with 15% silica gel. The catalyst with 10% silica gel exhibited the highest pore diameter. Larger pores facilitate improved access for reactant molecules, enhancing catalyst activity. Additionally, an optimal pore diameter is crucial for ensuring accessibility to active sites and maximizing the efficiency of chemical reactions (Wu et al., 2014). The porosity of the catalyst was tested by the N_2 physisorption method, resulting in a type IV isotherm curve with an H3-type hysteresis loop (Figure 2), which indicated the presence of mesopores with a pore width of more than 4 nm (Irwansyah et al., 2022). Type IV isotherms, indicative of mesoporous materials, demonstrate the phenomenon of capillary condensation of gas within the pores at specific pressure levels (Thommes et al., 2015). The pore sizes of silica gel, CaO, and CaO/silica gel catalysts (5%, 10%, and 15%) is in



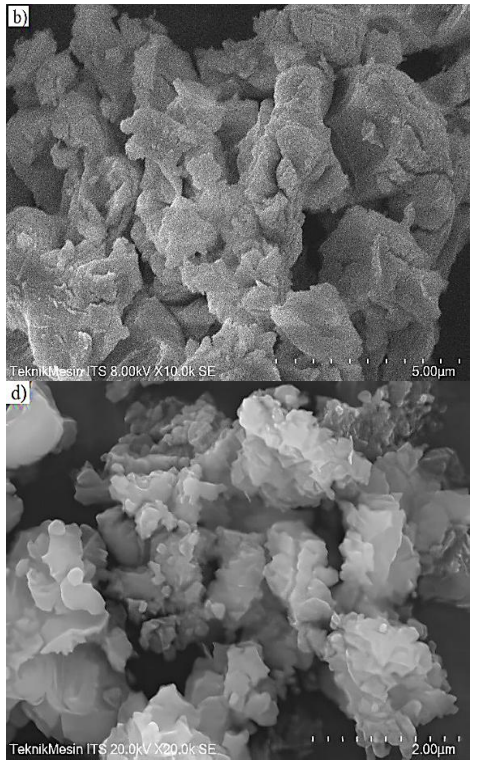


Fig. 3. SEM images of the catalysts (a) Silica gel, (b) CaO, (c) CaO/silica gel 5%, (d) CaO/silica gel 10%, and (e) CaO/silica gel 15%.

Table 5Biodiesel yields using CaO/silica gel 10% catalysts

		Independe	ent variable		- Observed biodiesel	Predicted biodiesel
No.	Reaction	Reaction Time	methanol-to-oil	Catalyst loading	Yield (%)	Yield (%)
	Temperature (°C)	(min)	molar ratio	(wt%)	riela (70)	1 leiu (70)
1	55 (-1)	60 (-1)	9 (-1)	1 (-1)	99.48	99.74
2	55 (-1)	60 (-1)	9 (-1)	2 (1)	96.46	96.52
3	55 (-1)	60 (-1)	15 (1)	1 (-1)	97.16	96.59
4	55 (-1)	60 (-1)	15 (1)	2 (1)	95.76	96.09
9	65 (1)	120 (1)	15 (1)	2 (1)	97.10	97.25
11	65 (1)	120 (1)	9 (-1)	2 (1)	95.40	95.51
12	65 (1)	120 (1)	9 (-1)	1 (-1)	95.20	95.27
16	65 (1)	60 (-1)	9 (-1)	1 (-1)	96.08	95.72
17	50 (-2)	90 (0)	12 (0)	1.5 (0)	97.32	96.04
18	60 (0)	30 (-2)	12 (0)	1.5 (0)	98.56	98.73
21	70 (2)	90 (0)	12 (0)	1.5 (0)	96.44	96.75
22	60 (0)	150 (2)	12 (0)	1.5 (0)	95.84	95.71
25	60 (0)	90 (0)	12 (0)	1.5 (0)	96.86	96.40
26	60 (0)	90 (0)	12 (0)	1.5 (0)	96.73	96.40
27	60 (0)	90 (0)	12 (0)	1.5 (0)	96.08	96.40
28	60 (0)	90 (0)	12 (0)	1.5 (0)	96.64	96.40
29	60 (0)	90 (0)	12 (0)	1.5 (0)	96.09	96.40
30	60 (0)	90 (0)	12 (0)	1.5 (0)	96.02	96.40

Table 6Model Summary Statistics CaO/silika gel 10%

Catalyst	Source	Std. Dev.	R²	Adjusted R ²	Predicted R ²	PRESS	
	Linear	2.00	0.1451	0.0084	-0.2988	151.38	
C=O /=:1:== ==1 100/	2FI	1.61	0.5761	0.3530	0.2879	83.00	
CaO/silica gel 10%	Quadratic	0.4339	0.9758	0.9532	0.8872	13.15	Suggested
	Cubic	0.4604	0.9873	0.9473	0.0490	110.84	Aliased

Table 7ANOVA data of experimental results using 10% CaO/silica gel catalysts

Source	Sum of Squares	df	Mean Square	F-value	p-value
Model	113.73	14	8.12	43.15	< 0.0001 (significant)
A-Temperature	0.1233	1	0.1233	0.6548	0.4310
B-Time	13.74	1	13.74	73.00	< 0.0001
C-Ratio	2.94	1	2.94	15.62	0.0013
D-Catalyst	0.1121	1	0.1121	0.5953	0.4524
AB	33.76	1	33.76	179.32	< 0.0001
AC	0.5041	1	0.5041	2.68	0.1226
AD	1.51	1	1.51	8.04	0.0125
BC	2.13	1	2.13	11.32	0.0043
BD	4.93	1	4.93	26.18	0.0001
CD	7.40	1	7.40	39.30	< 0.0001
A^2	0.4257	1	0.4257	2.26	0.1534
B ²	1.15	1	1.15	6.10	0.0260
C ²	15.65	1	15.65	83.15	< 0.0001
D^2	28.42	1	28.42	150.98	< 0.0001
Residual	2.82	15	0.1882		
Lack of Fit	2.10	10	0.2103	1.46	0.354 (not significant)
Pure Error	0.7209	5	0.1442		· · · · · · · · · · · · · · · · · · ·
Cor Total	116.55	29			

the range of 2–50 nm, classifying these materials as mesoporous.

3.4 Catalyst Morphology Analysis

The surface morphology of silica gel, CaO, and CaO/silica gel (5%, 10%, and 15%) was analyzed using Scanning Electron Microscopy (SEM), as shown in Figure 3. SEM shows that silica gel has a porous and agglomerated structure, with particles sticking together to form large micrometer-sized clusters. These particles vary in shape and size, suggesting a fairly wide size distribution and a natural agglomeration process during synthesis (Setyawan et al., 2021). These results are consistent

with homogeneous SiO_2 based silica gel, as reported by Pattanayak *et al.*, (2022). The morphology of CaO in Figure 3 (b) shows a layered structure with slab-shaped particles overlapping each other, creating an uneven surface.

The CaO particles have a fairly large size, around tens of micrometres, which leads to a low surface area, in accordance with the BET analysis results. In the CaO/silica gel catalysts (5%, 10%, and 15%), particle size variations were observed with some small particles of 1-2 μm and some large agglomerations of up to 10 μm . The CaO/silica gel 5% mixture showed an even distribution of particles with few agglomerations, micro-sized morphology, rough surface, and porous. This contributed to the

increase in specific surface area, as measured by BET. The addition of silica to the CaO catalyst increases the total pore volume, potentially increasing the number of active sites interacting with reactants, thus facilitating biodiesel formation (Wongjaikham *et al.*, 2023; Putra *et al.*, 2017). SEM images of the CaO/silica gel 10% blend show a slight increase in agglomeration but still maintain good porosity and surface roughness.

The addition of silica gel resulted in a surface area of 7.695 m²/g, showing a significant increase in surface area. In contrast, the CaO/silica gel 15% mixture showed more significant agglomeration with denser and clumpier particles, causing a decrease in porosity and specific surface area to 5.866 m²/g. This is due to the high agglomeration which closes the pores and forms large particles that reduce the accessible surface, in accordance with the findings of previous researchers (Manurung et al., 2023; Lani et al., 2017). The morphological changes observed through SEM greatly affect the specific surface area of the material measured using the BET method. At CaO/silica gel 10% composition, the optimal combination of particle distribution and porosity achieved the largest surface area. However, higher additions of silica gel cause agglomeration and pore closure, thus decreasing the specific surface area (Putra et al., 2017).

3.5 Biodiesel yield model design and analysis

This study investigated the parametric variables influencing biodiesel synthesis using analysis of variance and optimization through Response Surface Methodology (RSM) with the Design Expert-12 software. A total of 30 experiments were performed, and the factor levels were selected based on prior research findings (Krishnamurthy *et al.*, 2020).

$$Y = +96.40 - 0.0717A - 0.7567B - 0.3500C - 0.0683D + 1.45AB + 0.1775AC + 0.3075AD + 0.3650BC + 0.5550 + 0.6800CD + 0.1246A^2 + 0.2046B^2 - 0.7554C^2 - 1.02D^2$$
(2)

The data were analysed using multiple regression to derive a second-order polynomial equation, which was then evaluated for statistical significance (equation 2). Based on the Model Summary Statistics presented in Table 6, the cubic model was not recommended despite obtaining a good fit. The recommended model is the quadratic model, with the quadratic regression coefficients for CaO/silica gel 10% catalyst expressed in equations. A positive sign on the coefficient indicates a synergistic effect that increases biodiesel yield, while a negative sign indicates an antagonistic effect that decreases yield.

The variance analysis (ANOVA) results presented in Table 7 reveals that quadratic model for the catalyst is very significant, with an F-value of 43.15 and a P-value of < 0.0001. This indicates that the model effectively predicts biodiesel yield. A Pvalue of < 0.0001 signifies a significant influence of the independent variables on the yield of biodiesel, whereas a Pvalue of > 0.1 proposes an insignificant effect. The model's reliability is supported by the coefficient of determination (R2) and adjusted R2 values, which are 0.9758 and 0.9532, respectively, for the catalyst. An R2 value greater than 0.8 signifies a strong correlation between predicted and observed values, with values approaching 1.0 reflecting a better representation of the experimental data. Furthermore, a difference of less than 0.2 between the adjusted R2 and predicted R² indicates good predictive ability, minimal overfitting, and consistent model performance on both training

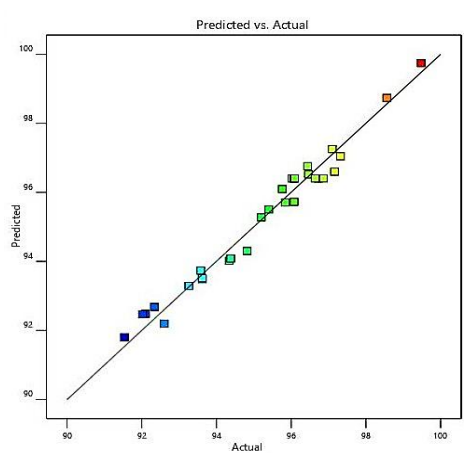


Fig. 4. Plot of predicted versus actual yield values of CaO/silica gel 10%

and unseen data. High R² and adjusted R² values indicate a strong relationship between the independent variables and the response, emphasizing the model's statistical significance and reliability (Chumuang & Punsuvon, 2017).

The parity plot in Figure 4 demonstrates strong agreement between the actual and predicted values, aligning closely with the 45° unit slope line, which reflects minimal error. The Adequate Precision ratio, representing the signal-to-noise ratio, was 32.541 for CaO/silica gel 5%, 25.891 for CaO/silica gel 10%, and 25.426 for CaO/silica gel 15%. These values indicate a sufficient signal for effective navigation of the design space. The F-value of 1.46 suggests an insignificant lack of fit, which is favourable as it confirms that the model fits the experimental data well. The CCD matrix used to determine the optimal combination of operating condition for maximizing the yield of biodiesel is shown in Table 5. For the CaO/silica gel 10% catalyst, the highest biodiesel yield, 99.48%, was achieved at the reaction conditions specified in experiment No. 1 in Table 5.

3.6 Effect of Process Conditions and Their Interactions on Biodiesel Yield

The interplay between the independent variables and the response variable was analyzed using three-dimensional (3D) surface plots, with the other variables held constant at their center values (0). The 3D surface plots illustrating biodiesel yield based on Equation (1) are presented in Figure 5, with color gradients ranging from blue to red, where red indicates the highest biodiesel yield. Figure 5(a) shows the effect of temperature (A) and reaction time (B) on biodiesel yield, with the catalyst weight of 1.5%, and the molar ratio of methanol to oil set at 12:1. Using the CaO/silica gel 10% catalyst, biodiesel yield predominantly ranged from 95% to 98%, peaking at 98% at temperatures between 55-57°C and a reaction time of 70 minutes. Beyond this point, the yield decreased slightly with prolonged reaction time. At temperatures between 57-61°C, the yield stabilized within 96-97%, and at 61-65°C, a slight reduction to around 97% was observed, particularly for shorter reaction times. Although higher temperatures slightly reduced the yield, the overall yield remained high. Reaction time had a more pronounced impact on biodiesel yield at lower temperatures, while at medium and high temperatures, its influence became minimal (Aibuedefe et al., 2023) .

Figure 5(b) illustrates the interaction between temperature and the oil/methanol ratio using the CaO/silica gel 10% catalyst. It seen that increasing both temperature and the

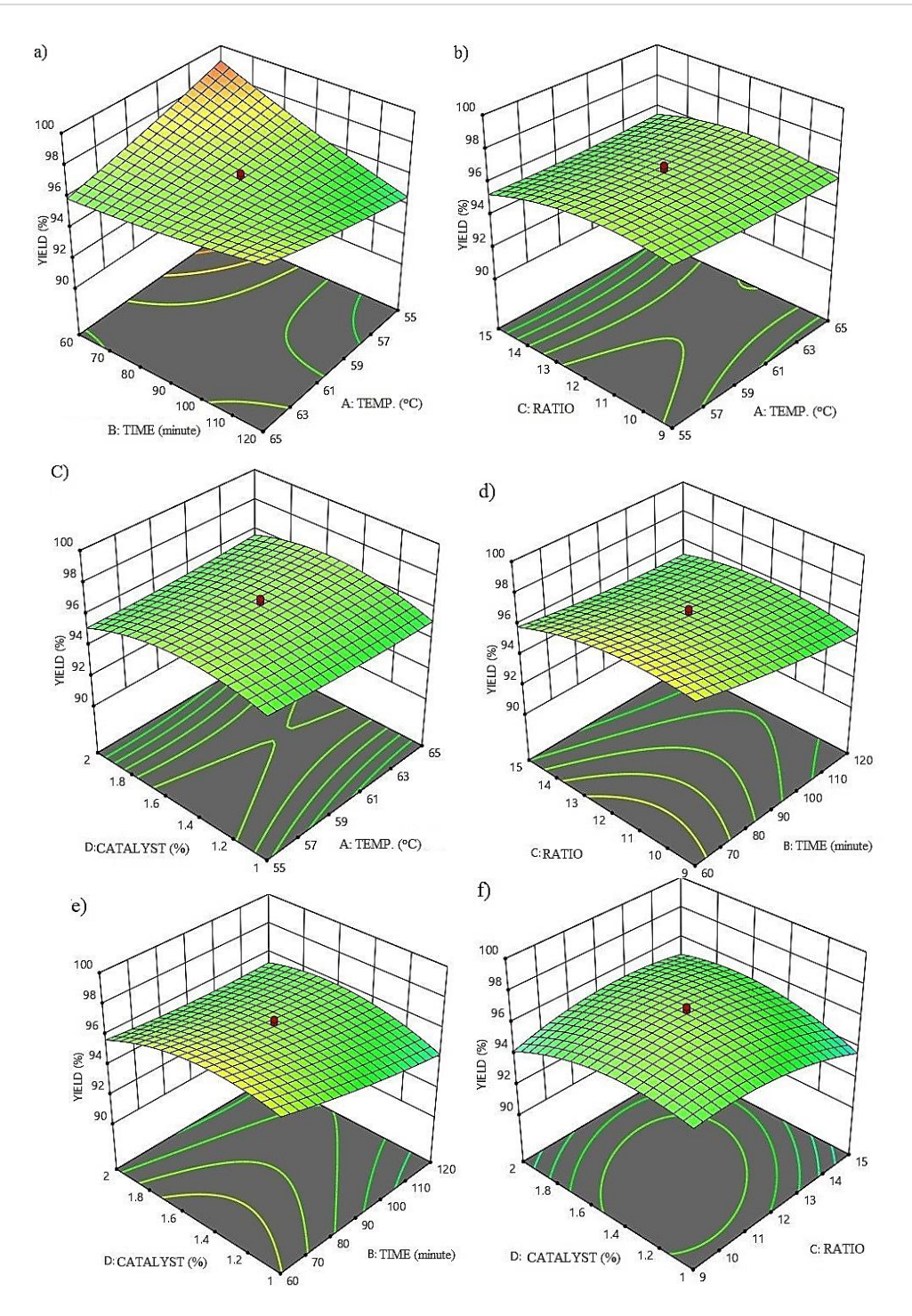


Fig. 5. Response surface plots that explain the effects of a) temperature and reaction time, b) temperature and oil/methanol mole ratio, c) temperature and catalyst amount, d) reaction time and oil/methanol mole ratio and catalyst amount.

oil/methanol ratio leads to a slight increase in biodiesel yield. The light green area on the graph, representing yields between 95.4% and 96.6%, indicates that changes in temperature and methanol ratio have minimal effect on the yields, which remain high and consistent. The 10% silica gel catalyst demonstrated good stability and tolerance to variations in reaction conditions, providing steady yields across a broad range of temperature and ratio combinations. Figure 5(c) depicts the interaction between temperature and catalyst amount, revealing that biodiesel yield remains stable between 95% and 96.5% within the temperature range of 55–65°C. Increasing both temperature and catalyst

percentage from 1% to 2% resulted in only a slight increase in yield, with the optimal zone observed at temperatures of 57–59°C and catalyst amounts of 1.4–1.6%, where the yield reached 96.5%. This suggests that the catalyst's response to variations in reaction conditions within this range is limited, likely due to the efficient utilization of its active sites (Buasri *et al.* 2024; Ahamed *et al.*, 2023).

Figure 5(d) illustrates the interaction between reaction time and the oil/methanol ratio on biodiesel yield using the CaO/silica gel 10% catalyst. At reaction times of 60-80 minutes, the yield ranged from 95% to 97%, with higher yields observed

at lower oil/methanol ratios (1:9–1:11). As the reaction time increased to 80–100 minutes, the yield stabilized at approximately 96–97%. However, at longer reaction times (110–120 minutes), the yield slightly decreased, particularly at higher oil/methanol ratios (1:13–1:15). The maximum yield was obtained with a reaction time of 60–70 minutes and an oil-to-methanol ratio ranging from 1:9 to 1:11. The catalyst remained stable and delivered high yields, especially at lower oil/methanol ratios, likely due to the optimal distribution and activity of the catalyst. This finding aligns with those reported by Aibuedefe *et al.* (2023), Ahmed *et al.* (2023), and Krishnamurthy *et al.* (2020).

Figure 5 (e) shows that the optimum biodiesel yield of 97% was achieved with a catalyst amount of 1.2-1.6% and a reaction time of 60-80 minutes. This maximum yield was achieved with a sufficient amount of catalyst in a short reaction time. At 1.4-1.8% catalyst and 90-100 minutes, the yield remained high (96%) but decreased slightly with increasing time and catalyst. Yield also tended to decrease at long reaction times with low catalyst (1.0-1.4%), indicating that long reaction times require adequate catalyst to remain efficient. Figure 5 (f) shows that the interaction of oil/methanol mole ratio and CaO/silica gel 10% catalyst amount resulted in a stable biodiesel yield between 94-96%. Mole ratios of 1:11 to 1:13 and catalyst amounts of 1.4-1.6% gave slightly higher yields of around 96%. Beyond this range, the yield only slightly decreased, with no significant improvement from further increasing the mole ratio or catalyst amount. This suggests that, for heterogeneous catalysts, a larger quantity of catalyst is needed to convert triglycerides into methyl esters. According to the study by Kolakoti et al. (2022), the amount of catalyst (wt%) was found to be a significant process variable, followed by the molar ratio.

3.7 Effect of silica content on biodiesel yield

The modification of the CaO catalyst with silica gel significantly enhanced biodiesel yield under the reaction conditions optimized by RSM at the centre point (temperature: 60°C, reaction time: 90 minutes, oil-to-methanol molar ratio: 1:12, catalyst weight: 1.5 g, and stirring speed: 500 rpm). Pure CaO yielded 89.85%. With the addition of 5% silica gel, the yield increased to 93.433%, attributed to the increased surface area from 1.032 m²/g to 6.097 m²/g, which provided more active sites (Lani *et al.*, 2017). The highest yield of 96.403% was obtained with 10% silica gel, where the catalyst's surface area, pore volume, and pore diameter were at optimal values, enhancing reactant diffusion and improving reaction efficiency (Wu *et al.*, 2014).

The catalyst modified with 10% silica gel exhibit an optimal balance of acidity (0.367 mmol/g) and basicity (20.8 mmol/g),

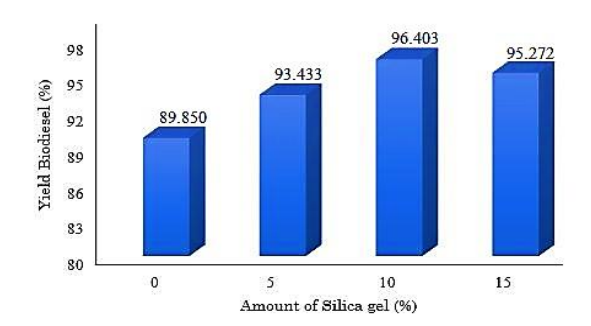


Fig. 6. Effect of silica content on biodiesel yield

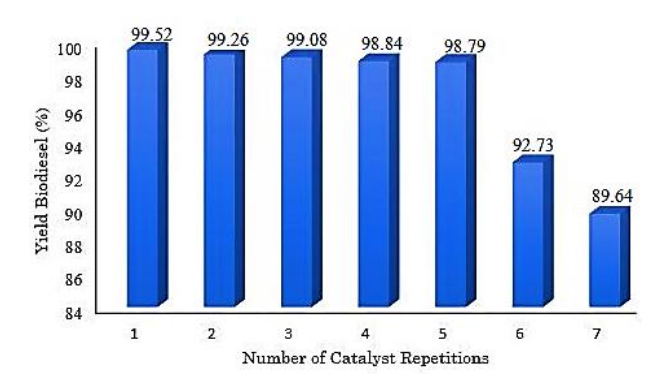


Fig. 7. Effect of catalyst reuse on biodiesel yield

which allowed the simultaneous activation of CPO and methanol, which facilitated a faster and more efficient reaction (Lani et al., 2020; Manurung et al., 2023). Silanol groups (Si-OH) on silica gel effectively converted the free fatty acid (FFA) content in the raw material through esterification reaction, while the basic side increased the transesterification efficiency (Wan Omar & Amin, 2011; Widayat et al 2017). The addition of silica gel beyond 10%, reaching 15%, resulted in a reduced biodiesel yield to 95.272%. This decrease is attributed to the excessive silica blocking active sites, reducing the surface area to 5.866 m²/g, and increasing the average crystal size to 30.479 nm (Lani et al., 2017). XRD analysis confirmed the formation of Ca₂SiO₄ due to interactions between silica and CaO, enhancing structural stability and catalytic properties. SEM analysis revealed an even distribution of silica, while BET results showed improved surface area and pore volume, facilitating the effective utilization of active sites. Consequently, a silica gel concentration of 10% is deemed optimal for achieving the highest biodiesel vield.

3.8 Effect of catalyst reuse on biodiesel yield

Catalyst reuse is a crucial factor in evaluating the stability and practicality of catalysts for biodiesel production in industrial applications. After the reaction, the catalyst was separated through filtration, dried at 70°C overnight, and subsequently retested. This procedure was carried out on the CaO/silica gel 5% catalyst under optimal conditions (catalyst weight 2 g, stirring speed 500 rpm, oil:methanol mole ratio 1:9, temperature 65°C, reaction time 60 minutes), with the results displayed in Figure 7. The findings reveal that up until the fifth reuse, the decrease in biodiesel yield was less than 1%, indicating that the catalyst remained stable and active, making it suitable for recycling in continuous industrial processes. However, by the sixth and seventh uses, a significant yield reduction was observed, from 98.79% to 92.73% and 89.63%, respectively. This decline is likely attributed to the leaching of Ca ions during the reaction, which diminishes the catalyst's activity (Lani et al., 2017), as well as potential contamination from oxygen, water, and carbon dioxide during the process (Huang et al., 2021).

3.9 Biodiesel characteristics

Characterization of the optimum biodiesel from each catalyst was conducted to evaluate its quality, which affects engine performance. Test parameters included water content, specific gravity, viscosity, residual carbon, and acid number, as shown in Table 8. The results were compared to the ASTM D6751 and EN 14214 standard (Inambao, 2023). The biodiesel produced from the CaO/silica gel catalysts (5%, 10%, and 15%) in this study showed quality characteristics in accordance with

Table 8
Comparison of biodiesel characterization results with biodiesel quality standard ASTM D6751 and EN 14214

		Biodi	Biodiesel from this study			
Parameter	ASTM D6751	CaO/silica gel 5%	CaO/silica gel 10%	CaO/silica gel 15%		
Methyl ester content (%)	96.5 (EN 14214)	99.04	99.21	98.22		
Water content (% v/v)	Max. 0.05	0.02	0.02	0.03		
Specific gravity 40°C (kg m ⁻³)	820-900	860	865	854		
Viscosity at 40°C (mm ² s ⁻¹)	1.9-6.0	3.3	3.4	3.9		
Carbon residue (%)	Max. 0.05	0	0	0		
Acid number (mg KOH/g)	Max. 0.5	0.9	0.8	1		

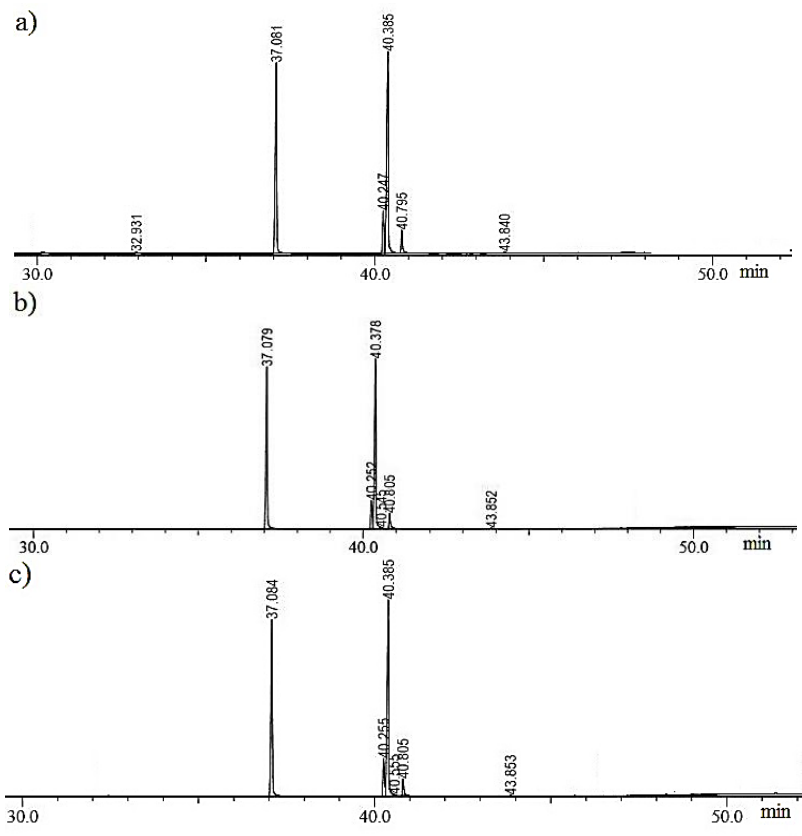


Fig. 8. GC-MS chromatograms of biodiesel using catalysts a) CaO/silica gel 5%, b) CaO/silica gel 10%, and c) CaO/silica gel 15%.

the standards, except for the acid number. The water content of the biodiesel from the three catalysts was 0.02%, 0.02%, and 0.03% (w/b), respectively, below the maximum limit of 0.05%. The specific gravity of biodiesel was recorded as 860, 865, and 854 kg/m³, respectively, which falls within the 850-890 kg/m³ range of the standard. The viscosity of the biodiesel was 3.3, 3.4, and 3.9 mm²/s, also within the standard (2.3-6.0 mm²/s). A carbon residue of 0% indicates complete combustion without residue (Mishra & Goswami, 2018). The acid number of the biodiesel exceeded the maximum standard of 0.5 mg-KOH/g, with values of 0.9, 0.8, and 1.0 mg-KOH/g, respectively. This discrepancy is due to the presence of minor compounds, such as oxalic acid, which increases the acidity of biodiesel. In addition, GC-MS analysis showed high methyl ester content of 99.04%, 99.21%, and 98.52% for 5%, 10%, and 15% CaO/silica gel catalysts, respectively, exceeding the minimum standard of 96.5%. Methyl palmitate and methyl oleate were the main components, as shown in Figure 8, and Tables 9. Reflects the optimal catalytic activity of the catalyst (Aibuedefe et al., 2023). These results indicate high quality biodiesel, although further

optimization is needed to lower the acid number to maintain engine performance and durability (Al-Muhtaseb et al., 2018).

3.10 Methyl ester content of biodiesel

GC-MS analysis was used to identify the methyl esters in the biodiesel samples. The chromatogram results of biodiesel at optimum conditions with 5%, 10%, and 15% CaO/silica gel catalysts are shown in Figure 8, with the types of methyl esters presented in Tables 9. The conversion of CPO to methyl esters was very high with methyl palmitate and methyl oleate dominating the analytical results, namely 99.04% for 5% catalyst, 99.21% for 10%, and 98.52% for 15%. The highest conversion on 10% catalyst was attributed to better catalytic activity due to modification of the catalyst surface (Aibuedefe *et al.*, 2023). Comparative GC-MS analysis showed all catalysts produced similar methyl ester profiles, with methyl oleate dominating (46.38% for 5%, 46.77% for 10%, and 46.79% for 15%) as well as methyl palmitate (39.02%; 40.27%; and 39.1% for 5%, 10%, and 15%).

Table 9Results of methyl ester type analysis in biodiesel products using CaO/silica gel (5%, 10% and 15%) catalyst

Retention time	Mathal astantana	Molecular Formula	Composition (%)			
Retention time	Methyl ester type	Molecular Formula	CaO/silica gel 5%	CaO/silica gel 10%	CaO/silica gel 15%	
32.931	Methyl myristate	C ₁₅ H ₃₀ O ₂	0.35	-	-	
37.081	Methyl palmitate	$C_{17}H_{34}O_2$	39.02	40.27	39.1	
40.247	Methyl linoleate	$C_{19}H_{34}O_2$	8.48	7.59	8.5	
40.385	Methyl oleate	$C_{19}H_{36}O_2$	46.38	46.77	46.79	
40.545	Methyl elaidate	$C_{19} H_{36} O_2$	-	0.04	-	
40.555	Methyl octadecanoate	$C_{19}H_{36}O_2$	-	-	0.03	
40.795	Methyl stearate	$C_{19}H_{38}O_2$	4.54	4.3	3.85	
43.840	Methyl arachidate	$C_{21}H_{42}O_2$	0.27	0.24	0.25	
· ·	TOTAL		99.04	99.21	98.52	

4. Conclusion

This study demonstrated the application of CaO/silica gel heterogeneous catalyst synthesized from biomass waste effectively converted crude palm oil into biodiesel. The incorporation of silica gel into the CaO catalyst enhanced its surface area and stability, with the amount of 10% silica gel catalyst achieving a biodiesel yield of 96.4% under reaction conditions of 65°C, 60 minutes, and an oil-to-methanol molar ratio of 1:9. The optimization using Response Surface Methodology (RSM) has identified the temperature as the most influential factor in maximizing the yield. The optimum biodiesel yield of 99.52% was achieved using a 5% CaO/silica gel catalyst under the same reaction conditions, demonstrating the potential of this catalyst for efficient biodiesel production. The 5% CaO/silica gel catalyst demonstrated excellent stability, maintaining consistent biodiesel yields over five reuse cycles, highlighting its potential for industrial applications. The biodiesel produced met ASTM D6751 and EN 14214 standards, except for a slightly elevated acid number. Notably, the 10% CaO/silica gel catalyst achieved the highest methyl ester purity at 99.98%. This study underscores the significant potential of biomass waste-derived catalysts, such as CaO/silica gel, in promoting environmentally friendly and efficient biodiesel production.

Acknowledgements

Authors gratefully acknowledged to the Ministry of Research and Technology, Indonesian Directorate General of Higher Education (DRTPM) through the LPPM Riau University under Research Thesis Magister Grant for the financial support of this project (Contract No. 20760/UN19.5.1.3/AL.04/2024).

References

- Ahamed, M. S., Lingfa, P., & Chandrasekaran, M. (2023). RSM modelling and optimization for performance evaluation of biodiesel production process from livistona jenkinsiana using NaOH as a catalyst. *Engineering Research Express*, 5(4). https://doi.org/10.1088/2631-8695/ad069b
- Ahmed, M., Ahmad, K. A., Vo, D.-V. N., Yusuf, M., Haq, A., Abdullah, A., Aslam, M., Patle, D. S., Ahmad, Z., Ahmad, E., & Athar, M. (2023). Recent trends in sustainable biodiesel production using heterogeneous nanocatalysts: Function of supports, promoters, synthesis techniques, reaction mechanism, and kinetics and thermodynamic studies. *Energy Conversion and Management*, 280, 116821. https://doi.org/10.1016/j.enconman.2023.116821
- Aibuedefe, F., Osaro, K., & Tina, E. (2023). Sustainable Chemistry for the Environment Process optimization for blended waste frying oil in biodiesel production using CaO derived from African

- periwinkle shell catalyst through response surface methodology. *Sustainable Chemistry for the Environment*, 4(March), 100042. https://doi.org/10.1016/j.scenv.2023.100042
- Ajala, E. O., Ajala, M. A., Ajao, A. O., Saka, H. B., & Oladipo, A. C. (2020).

 Calcium-carbide residue: A precursor for the synthesis of CaO–Al2O3–SiO2–CaSO4 solid acid catalyst for biodiesel production using waste lard. *Chemical Engineering Journal Advances*, 4(October), 100033. https://doi.org/10.1016/j.ceja.2020.100033
- Al-Muhtaseb, A. H., Jamil, F., Al-Haj, L., Zar Myint, M. T., Mahmoud, E., Ahmad, M. N. M., Hasan, A. O., & Rafiq, S. (2018). Biodiesel production over a catalyst prepared from biomass-derived waste date pits. *Biotechnology Reports*, 20. https://doi.org/10.1016/j.btre.2018.e00284
- Alhadhrami, A., Mohamed, G. G., Sadek, A. H., Ismail, S. H., Ebnalwaled, A. A., & Almalki, A. S. A. (2022). Behavior of Silica Nanoparticles Synthesized from Rice Husk Ash by the Sol–Gel Method as a Photocatalytic and Antibacterial Agent. *Materials*, 15(22). https://doi.org/10.3390/ma15228211
- Anuar, M. F., Fen, Y. W., Zaid, M. H. M., Matori, K. A., & Khaidir, R. E. M. (2020). The physical and optical studies of crystalline silica derived from the green synthesis of coconut husk ash. *Applied Sciences* (Switzerland), 10(6). https://doi.org/10.3390/app10062128
- Ayoola, A. A., Hymore, F. K., Omonhinmin, C. A., Babalola, P. O., Fayomi, O. S. I., Olawole, O. C., Olawepo, A. V., & Babalola, A. (2020). Response surface methodology and artificial neural network analysis of crude palm kernel oil biodiesel production. *Chemical Data Collections*, 28. https://doi.org/10.1016/j.cdc.2020.100478
- Buasri, A., Kamsuwan, J., Dokput, J., Buakaeo, P., Horthong, P., & Loryuenyong, V. (2024). Green synthesis of metal oxides (CaO-K2O) catalyst using golden apple snail shell and cultivated banana peel for production of biofuel from non-edible Jatropha Curcas oil (JCO) via a central composite design (CCD). *Journal of Saudi Chemical Society*, 28(3), 101836. https://doi.org/10.1016/j.jscs.2024.101836
- Chumuang, N., & Punsuvon, V. (2017). Response Surface Methodology for Biodiesel Production Using Calcium Methoxide Catalyst Assisted with Tetrahydrofuran as Cosolvent. Journal of Chemistry, 2017. https://doi.org/10.1155/2017/4190818
- Ghadafi, M., Santosa, S. J., Kamiya, Y., & Nuryono, N. (2020). Free na and less fe compositions of SiO2 extracted from rice husk ash as the silica source for synthesis of white mineral trioxide aggregate. *Key Engineering Materials*, 840 KEM, 311–317. https://doi.org/10.4028/www.scientific.net/kem.840.311
- Hadiyanto, H., Lestari, S.P., Abdullah, A., Widayat, W., Sutanto, H. (2016). The development of fly ash-supported CaO derived from mollusk shell of Anadara granosa and Paphia undulata as heterogeneous CaO catalyst in biodiesel synthesis. *International Journal of Energy and Environmental Engineering*, 7(3), 297–305. https://doi.org/10.1007/s40095-016-0212-6
- Haryono, H., Ishmayana, S., & Fauziyah, I. (2023). Synthesis and Characterization of Calcium Oxide Impregnated on Silica from Duck Egg Shells and Rice Husks as Heterogeneous Catalysts for Biodiesel Synthesis. *Baghdad Science Journal*, 20, 1976–1984.

https://doi.org/10.21123/bsj.2023.7895

- Helwani, Z., Ramli, M., Saputra, E., Bahruddin, B., Yolanda, D., Fatra, W., Idroes, G. M., Muslem, M., Mahlia, T. M. I., & Idroes, R. (2020). Impregnation of CaO from eggshell waste with magnetite as a solid catalyst (Fe3O4/CaO) for transesterification of palm oil off-grade. *Catalysts*, 10(2), 1–13. https://doi.org/10.3390/catal10020164
- Hoekman, S. K., Broch, A., Robbins, C., Ceniceros, E., & Natarajan, M. (2012). Review of biodiesel composition, properties, and specifications. *Renewable and Sustainable Energy Reviews*, 16(1), 143–169. https://doi.org/10.1016/j.rser.2011.07.143
- Huang, J., Zou, Y., Yaseen, M., Qu, H., He, R., & Tong, Z. (2021). Fabrication of hollow cage-like CaO catalyst for the enhanced biodiesel production via transesterification of soybean oil and methanol. Fuel, 290, 119799. https://doi.org/10.1016/j.fuel.2020.119799
- Inambao, F. (2023). Biodiesel Standards and Quality Testing: A Review. Journal of Harbin Engineering University, 44(10), 273–295. https://harbinengineeringjournal.com/index.php/journal/article/view/1508
- Irwansyah, F. S., Amal, A. I., Diyanthi, E. W., Hadisantoso, E. P., Noviyanti, A. R., Eddy, D. R., & Risdiana, R. (2022). How to Read and Determine the Specific Surface Area of Inorganic Materials using the Brunauer-Emmett-Teller (BET) Method. *ASEAN Journal of Science and Engineering*, 4(1), 61–70. https://doi.org/10.17509/ajse.v4i1.60748
- Kedir, W. M., Wondimu, K. T., & Weldegrum, G. S. (2023). Optimization and characterization of biodiesel from waste cooking oil using modified CaO catalyst derived from snail shell. *Heliyon*, 9(5), e16475. https://doi.org/10.1016/j.heliyon.2023.e16475
- Kolakoti, A., Setiyo, M., & Rochman, M. L. (2022). A Green Heterogeneous Catalyst Production and Characterization for Biodiesel Production using RSM and ANN Approach. International Journal of Renewable Energy Development, 11(3), 703–712. https://doi.org/10.14710/ijred.2022.43627
- Krishnamurthy, K. N., Sridhara, S. N., & Ananda Kumar, C. S. (2020). Optimization and kinetic study of biodiesel production from Hydnocarpus wightiana oil and dairy waste scum using snail shell CaO nano catalyst. *Renewable Energy*, *146*, 280–296. https://doi.org/10.1016/j.renene.2019.06.161
- Lani, N. S., Ngadi, N., & Inuwa, I. M. (2020). New route for the synthesis of silica-supported calcium oxide catalyst in biodiesel production. *Renewable Energy*, 156, 1266–1277. https://doi.org/10.1016/j.renene.2019.10.132
- Lani, N. S., Ngadi, N., Yahya, N. Y., & Rahman, R. A. (2017). Synthesis, characterization and performance of silica impregnated calcium oxide as heterogeneous catalyst in biodiesel production. *Journal of Cleaner Production*, 146, 116–124. https://doi.org/10.1016/j.jclepro.2016.06.058
- Maisarah, Nurhayati, & Linggawati, A. (2020). Transesterification of Crude Palm Oil (CPO) to Biodiesel Using Heterogeneous Catalyst K-CaO from Anadara Granosa Synthesized by Sol Gel Method. *Journal of Physics: Conference Series*, 1655(1). https://doi.org/10.1088/1742-6596/1655/1/012035
- Manurung, R., Parinduri, S. Z. D. M., Hasibuan, R., Tarigan, B. H., & Siregar, A. G. A. (2023). Synthesis of nano-CaO catalyst with SiO2 matrix based on palm shell ash as catalyst support for one cycle developed in the palm biodiesel process. *Case Studies in Chemical and Environmental Engineering*, 7, 100345. https://doi.org/10.1016/j.cscee.2023.100345
- Mishra, V. K., & Goswami, R. (2018). A review of production, properties and advantages of biodiesel. *Biofuels*, 9(2), 273–289. https://doi.org/10.1080/17597269.2017.1336350
- Norul Azlin, M. Z., & Syamim Syufiana, S. (2022). The preparation and characterization of silica from coconut husk. *Journal of Physics: Conference Series*, 2266(1). https://doi.org/10.1088/1742-6596/2266/1/012011
- Nurhayati, Amri, T. A., Annisa, N. F., & Syafitri, F. (2020). The Synthesis of Biodiesel from Crude Palm Oil (CPO) using CaO Heterogeneous Catalyst Impregnated H2SO4, Variation of Stirring Speed and Mole Ratio of Oil to Methanol. *Journal of Physics: Conference Series*, 1655. https://doi.org/10.1088/1742-6596/1655/1/012106
- Ooi, H. K., Koh, X. N., Ong, H. C., Lee, H. V., Mastuli, M. S., Taufiq-Yap,

- Y. H., Alharthi, F. A., Alghamdi, A. A., & Mijan, N. A. (2021). Progress on modified calcium oxide derived waste-shell catalysts for biodiesel production. *Catalysts*, *11*(2), 1–26. https://doi.org/10.3390/catal11020194
- Osman, N. S., & Apawe, N. (2020). Synthesis of silica (SiO2) from reproducible acid-leached oil palm frond ash (OPFA) via optimized sol-gel method. *Materials Today: Proceedings*, *31*, 249–252. https://doi.org/10.1016/j.matpr.2020.05.330
- Ozor, P. A., Aigbodion, V. S., & Sukdeo, N. I. (2023). Modified calcium oxide nanoparticles derived from oyster shells for biodiesel production from waste cooking oil. *Fuel Communications*, *14*, 100085. https://doi.org/10.1016/j.jfueco.2023.100085
- Pandiangan, K. D., Simanjuntak, W., Ilim, I., Satria, H., & Jamarun, N. (2019). Catalytic Performance of CaO/SiO2 Prepared from Local Limestone Industry and Rice Husk Silica. *The Journal of Pure and Applied Chemistry Research*, 8(2), 170–178. https://doi.org/10.21776/ub.jpacr.2019.008.02.459
- Pattanayak, D. K., Muduli, J., Sahu, S. S., Gouda, S., Meher, S., Dash, T., Rout, S., & Pattnaik, P. K. (2022). Production and Characterization of Amorphous Silica Nanoparticles from Coconut Shell and Coir. Letters in Applied NanoBioScience, 11(4), 4040–4049. https://doi.org/10.33263/LIANBS114.40404049
- Putra, M. D., Ristianingsih, Y., Jelita, R., Irawan, C., & Nata, I. F. (2017). Potential waste from palm empty fruit bunches and eggshells as a heterogeneous catalyst for biodiesel production. *RSC Advances*, 7(87), 55547–55554. https://doi.org/10.1039/c7ra11031f
- Setyawan, N., Hoerudin, & Yuliani, S. (2021). Synthesis of silica from rice husk by sol-gel method. IOP Conference Series: Earth and Environmental Science, 733(1). https://doi.org/10.1088/1755-1315/733/1/012149
- Simpen, I. N., Negara, I. M. S., & Ratnayani, O. (2021).

 KARAKTERISTIK FISIKO-KIMIA KATALIS HETEROGEN
 CaO-BASE DAN PEMANFAATANNYA UNTUK KONVERSI
 MINYAK GORENG BEKAS SECARA SINAMBUNG MENJADI
 BIODIESEL. Jumal Kimia, 15(2), 188.
 https://doi.org/10.24843/jchem.2021.v15.i02.p09
- Sofyan, M. I., Mailani, P. J., Setyawati, A. W., Sulistia, S., Suciati, F., Hauli, L., Putri, R. A., Ndruru, S. T. C. L., Mawarni, R. S., Meliana, Y., Nurhayati, N., & Joelianingsih, J. (2024). Use of Sulfuric Acid-Impregnated Biochar Catalyst in Making of Biodiesel from Waste Cooking Oil via Leaching Method. *Bulletin of Chemical Reaction Engineering and Catalysis*, 19(1), 160–170. https://doi.org/10.9767/bcrec.20113
- Thommes, M., Kaneko, K., Neimark, A. V., Olivier, J. P., Rodriguez-Reinoso, F., Rouquerol, J., & Sing, K. S. W. (2015). Physisorption of gases, with special reference to the evaluation of surface area and pore size distribution (IUPAC Technical Report). *Pure and Applied Chemistry*, 87(9–10), 1051–1069. https://doi.org/10.1515/pac-2014-1117
- Wan Omar, W. N. N., & Amin, N. A. S. (2011). Biodiesel production from waste cooking oil over alkaline modified zirconia catalyst. *Fuel Processing Technology*, 92(12), 2397–2405. https://doi.org/10.1016/j.fuproc.2011.08.009
- Wirawan, S. S., Solikhah, M. D., Setiapraja, H., & Sugiyono, A. (2024). Biodiesel implementation in Indonesia: Experiences and future perspectives. *Renewable and Sustainable Energy Reviews*, 189(PA), 113911. https://doi.org/10.1016/j.rser.2023.113911
- Wongjaikham, W., Kamjam, M., Wongsawaeng, D., Ngaosuwan, K., Kiatkittipong, W., Hosemann, P., & Assabumrungrat, S. (2023). Heterogeneously catalyzed palm biodiesel production in intensified fruit blender. *Arabian Journal of Chemistry*, 16(11), 105273. https://doi.org/10.1016/j.arabjc.2023.105273
- Widayat, W., Darmawan, T., Hadiyanto, H., Rosyid, R.Ar.(2017).Preparation of Heterogeneous CaO Catalysts for Biodiesel Production. *Journal of Physics: Conference Series*, 877(1), 012018. https://doi.org/10.1088/1742-6596/877/1/012018
- Wu, H., Zhang, J., Liu, Y., Zheng, J., & Wei, Q. (2014). Biodiesel production from Jatropha oil using mesoporous molecular sieves supporting K2SiO3 as catalysts for transesterification. Fuel Processing Technology, 119, 114–120. https://doi.org/10.1016/j.fuproc.2013.10.021
- Zuwanna, I., Riza, M., Aprilia, S., Syamsuddin, Y., & Dewi, R. (2023).
 Preparation and characterization of silica from rice husk ash as a reinforcing agent in whey protein isolate biocomposites film.

South African Journal of Chemical Engineering, 44(August 2022),

337–343. https://doi.org/10.1016/j.sajce.2023.03.005



© 2025. The Author(s). This article is an open access article distributed under the terms and conditions of the Attribution-ShareAlike 4.0 (CC BY-SA) International License (http://creativecommons.org/licenses/by-sa/4.0/) © 2025. The Author(s). This article is an open access article distributed under the terms and conditions of the Creative Commons